Efficient Realization of Wave Digital Components for Physical Modeling and Sound Synthesis

Matti Karjalainen, *Senior Member, IEEE*

***Abstract*—Wave digital filters (WDFs) were originally developed for robust discrete-time simulation of analog filters, but recently they have been applied successfully to modeling of physical systems such as musical instruments and to model-based sound synthesis. While basic WDF elements are sufficient to implement arbitrary passive lumped-element models, the computational efficiency of such models is not optimal. In this paper, we explore methods to realize consolidated impedance or admittance wave ports that are compatible to WDFs and digital waveguides. In addition to efficiency, attention is paid to simplicity of parametric control. A modeling and sound synthesis case study of the bell is presented to demonstrate the performance obtained by the consolidated approach.**

***Index Terms*—Physical modeling, sound synthesis, wave digital filters (WDFs).**

I. Introduction

PHYSICS-BASED modeling and sound synthesis of musical instruments have successfully exploited wave-based simulation and synthesis methods, particularly digital waveguides (DWGs) and wave digital filters (WDFs) [1]–[3]. Cases of WDF models are published for example in [4]–[9]. While DWGs focus on modeling of wave propagation delays and wave scattering at junctions of waveguide branches [1], WDFs were formulated to simulate lumped element circuits and networks [10]. The use of wave variables (W-variables) in WDFs and DWGs contrasts to simulation using Kirchhoff variables (K-variables) as directly observable physical quantities, such as voltage and current in the electrical domain, force and velocity in the mechanical domain, or pressure and volume velocity in the acoustical domain.

The WDF theory provides a compact set of basic blocks to construct models composed of lumped elements. WDFs are known to be numerically robust [10]–[14] as well as extensible to simulate nonlinear [3], [8], [9], [15], [16] and multidimensional systems [3]. These elements are connected through wave ports to form circuits and networks, which in linear and time-invariant (LTI) cases is a straightforward task by using multiport adaptors for the connections.

Although being a general and modular approach, classical WDF models made of basic elements are not optimal from the point of view of computational efficiency. Furthermore, for complex physical subsystems that are not specified by analog circuit elements, this may not be a practical way of modeling. Computational efficiency is a crucial factor in real-time sound synthesis. When the stability and numerical robustness requirements of a model are fulfilled, which is often easily checked for a particular realization, efficiency is the main factor. Even small improvement can help making a specific application computable in real-time. Currently, a large part of physics-based modeling and sound synthesis is made as software for general-purpose computers or signal processors, where efficient floating-point support is available and numerical accuracy is often no problem. This has been the starting point and motivation for the formulation of the "consolidated" wave digital components presented in this paper.

The idea of consolidated WDF compatible components, i.e., realizing a circuit or a subcircuit as a single digital filter for wave port reflectance function, is obvious and not new. For a given realizable impedance, any standard infinite-impulse response (IIR) [and sometimes finite-impulse response (FIR)] filter structure can be used as far as numerical robustness requirements are fulfilled. Extensions to the basic WDF theory that try to accommodate similar principles are given for example in [16]–[19]. None of them has, however, presented a systematic derivation of filter structures that focus on maximizing computational efficiency, yet being numerically robust enough. The concept of efficiency here includes the sample-by-sample speed of signal flow but also the computation of parameters for time-varying filters, which is frequently carried out at a lower control rate in order to improve overall efficiency. The filter structures for port reflectance presented in this paper try to meet these objectives.

The content of the paper is as follows. Section II is an overview of WDF fundamentals and considered helpful, since few people in audio digital signal processing (DSP) are familiar enough with the topic, and classical references are somewhat difficult to read without circuit theory background. A systematic approach to build consolidated WDF wave-port components in a computationally efficient manner is presented in Section III. Implementation issues, computational efficiency, and simplicity of parametric control in particular, are analyzed in Section IV. An example of WDF modeling using the proposed methods is given in Section V, and the paper is concluded by a discussion and conclusions.

II. Classical WDF Components and Structures

In order to provide necessary background for consolidated wave digital components, an overview of the most basic WDF elements and construction of network models is summarized in this section. We concentrate on passive lumped LTI elements and adaptors that are used for element connections [10]. Fig. 1 illustrates a set of such components related to the electrical

Manuscript received October 7, 2007; revised March 28, 2008. This work was supported by the Academy of Finland under Project 106956. The associate editor coordinating the review of this manuscript and approving it for publication was Dr. Rudolf Rabenstein.

The author is with the Department of Signal Processing and Acoustics, Helsinki University of Technology, FI-02015 TKK, Finland (e-mail: matti.karjalainen@tkk.fi).

Digital Object Identifier 10.1109/TASL.2008.924155

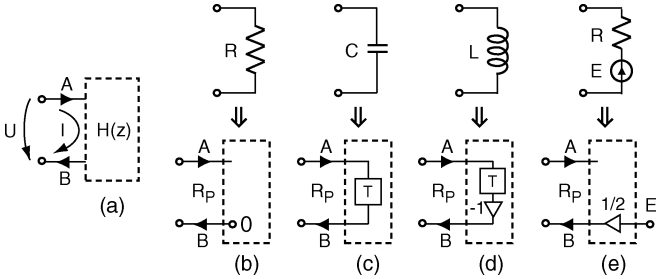

Fig. 1. Definition of basic WDF one-port elements. (a) A generic one-port, (b) resistor: $R_\mathrm{p} = R$, (c) capacitor: $R_\mathrm{p} = T/2C$, (d) inductor: $R_\mathrm{p} = 2L/T$, (e) voltage source: $R_\mathrm{p} = R$, where C, L, and R are physical capacitance, inductance, and resistance, respectively, and T is unit delay.

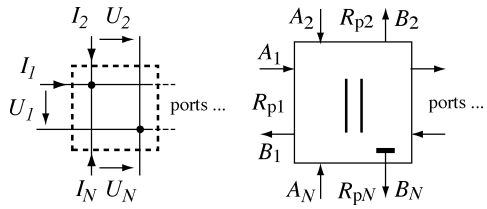

Fig. 2. Parallel adaptor: (left) connection for K-variables, (right) corresponding WDF symbol for wave variable, including reflection-free port N marked by signal terminal symbol $\top$.

domain. Both electrical symbols and corresponding WDF realizations are depicted. Due to the analogies between physical domains, similar elements can be defined for example for the mechanical and the acoustical domains.

A. Passive One-Port Elements

Fig. 1(a) characterizes a generic LTI one-port element in the electrical domain, for which the K-variables are voltage u and current i. The WDF theory maps these to (voltage) wave variables a and b at the port by relations[1]

$$\begin{cases} u = a + b \\ i = (a - b)/R_\mathrm{p} \end{cases} \Leftrightarrow \begin{cases} a = (u + R_\mathrm{p} i)/2 \\ b = (u - R_\mathrm{p} i)/2 \end{cases} \tag{1}$$

where a is the incident (incoming) and b the reflected (outgoing) wave component as specified in Fig. 1(a), and R_p is a free parameter called port resistance. While the relation between the two K-variables in a linear system is given by impedance $Z = U/I$ (capital letters from now on denote Laplace or z-transform domain variables), the behavior of a wave port is described by its reflectance

$$H = \frac{B}{A} = \frac{Z - R_\mathrm{p}}{Z + R_\mathrm{p}}. \tag{2}$$

Wave digital filters are derived from analog prototypes by the bilinear mapping [20]

$$s = \frac{2}{T} \cdot \frac{z-1}{z+1} \quad \Leftrightarrow \quad z = \frac{1 + sT/2}{1 - sT/2} \tag{3}$$

where $s = \alpha + j\omega$ is the complex-valued Laplace transform variable with angular frequency ω, T is the sample period, and z is the discrete-time z-transform variable. This mapping corresponds to using the trapezoidal rule in numerical integration. The bilinear transform preserves energetic properties of the prototype analog system such as passivity, which is important from the stability point of view. A practical problem with the bilinear transform is that the frequency axis is warped by the rule

$$\omega = -j\frac{2}{T}\frac{e^{j\hat{\omega}T} - 1}{e^{j\hat{\omega}T} + 1} = \frac{2}{T}\tan\left(\frac{\hat{\omega}T}{2}\right) \tag{4}$$

[1]This deviates from the traditional definition [10] by a scaling factor of 1/2 in order to make the WDF wave variables physically normalized and directly compatible to DWG ports. This scaling has no effect to the formulations below except in the voltage source of Fig. 1(e).

so that going to the limit $\omega \to \infty$ in analog angular frequency ω is mapped to approaching the Nyquist frequency, i.e., $\hat{\omega}T \to \pi$ of the discrete-time angular frequency $\hat{\omega}$. This warping problem can be severe in audio applications where the full Nyquist range needs to be realized accurately. Oversampling is one way to alleviate the problem, being however computationally expensive: oversampling by a factor of eight is needed to reduce the frequency warping effect down to about 1% in the baseband. Another way to counteract the problem is to use prewarping in filter design [21], but this is often difficult or impossible for the complex filter structures needed in physics-based modeling.

Based on (2) and (3) and by selecting proper values for the port resistance R_p, realizations of basic WDF elements are easily derived [10]. Although the port resistance R_p is in principle a free parameter, it must be selected in a specific way to make WDF models computable without delay-free loops.

In the electrical domain, a *resistor* with resistance $R = U/I$ is realized simply by selecting $R_\mathrm{p} = R$ so that reflectance $H = 0$ and $B = 0$; see Fig. 1(b).

For a *capacitor* with capacitance C the impedance in the Laplace domain is $Z_\mathrm{C}(s) = 1/sC$, which bilinearly maps to z-domain impedance $Z(z) = (T/2C)(1 + z^{-1})/(1 - z^{-1})$. Delay-free loops are avoided by selecting $R_\mathrm{p} = T/2C$, and the reflectance becomes simply a unit delay $H_\mathrm{C}(z) = z^{-1}$; see Fig. 1(c).

Respectively, for an *inductor* with inductance L, $Z_\mathrm{L}(s) = sL$, the port resistance is selected as $R_\mathrm{p} = 2L/T$, and the reflectance becomes $H_\mathrm{L}(z) = -z^{-1}$; see Fig. 1(d).

A *voltage source* with open-circuit voltage E and source resistance R can be derived to correspond to Fig. 1(e) with $R_\mathrm{p} = R$. The coefficient 1/2 becomes from the scaling convention used in (1).

B. Adaptors

Adaptors are WDF multiport elements that are needed to construct circuit and network models from the basic elements by parallel and series connections. The task of an adaptor is to realize the scattering of wave variables among the ports connected together.

For a parallel connection of circuit elements (Fig. 2) the Kirchhoff laws state that the voltages U_n at the ports $n = 1, \ldots, N$ must be equal and the sum of currents I_n must be zero, i.e.,

$$U_n = U_\mathrm{par} \quad \text{and} \quad \sum_{n=1}^{N} I_n = 0. \tag{5}$$

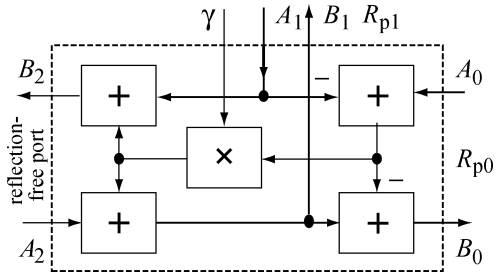

Fig. 3. Three-port parallel adaptor with a reflection-free port.

By eliminating K-variables and expressing the behavior in wave variables, we get scattering rules for an N-port *parallel adaptor*

$$B_n = \left(\sum_{k=1}^{N} \gamma_k A_k\right) - A_n \quad \text{and} \quad \gamma_k = 2G_k / \sum_{i=1}^{N} G_i \qquad (6)$$

where $G_i = 1/R_i$ are port conductances. Parameters γ_k are wave scattering coefficients. It can be readily seen that $\sum_{k=1}^{N} \gamma_k = 2$. An important special case is to select a single port, say port N, so that $G_N = \sum_{n=1}^{N-1} G_n$, whereby $\gamma_N = 1$ and for $n = 1, \ldots, N$ we can write

$$\gamma_n = G_n / G_N \qquad (7)$$

$$B_N = \sum_{n=1}^{N-1} \gamma_n A_n \qquad (8)$$

$$B_n = B_N + A_N - A_n \qquad (9)$$

which makes port N output B_N independent of its input A_N. This is called a *reflection-free port* because B_N can be read before knowing the new value of A_N, which cannot be done for the other ports. Such reflection-free port can be used without computability problems for further connections in a network in a way similar to one-port elements; see II-C.

Adaptors are often used as three-port elements. Fig. 3 shows a computationally optimized three-port parallel adaptor [10].

A *series adaptor* is derived correspondingly from Kirchhoff equations

$$I_n = I_{\text{ser}} \quad \text{and} \quad \sum_{n=1}^{N} U_n = 0 \qquad (10)$$

i.e., the currents I_n at the ports must be equal and the sum of voltages U_n around the series connection must be zero. For wave variables, this yields

$$B_k = A_k - \gamma_k \sum_{n=1}^{N} A_n \quad \text{and} \quad \gamma_k = 2R_k / \sum_{n=1}^{N} R_n. \qquad (11)$$

As for the parallel adaptor, a reflection-free port is achieved by making the corresponding scattering coefficient γ equal to 1. For example, for port N (Fig. 4), we can select $R_N = \sum_{n=1}^{N-1} R_n$, whereby $\gamma_N = 1$ and for $n = 1, \ldots, N$ we can write

$$\gamma_n = R_n / R_N \qquad (12)$$

$$B_N = -\sum_{n=1}^{N-1} A_n \qquad (13)$$

$$B_n = A_n - \gamma_n (A_N - B_N). \qquad (14)$$

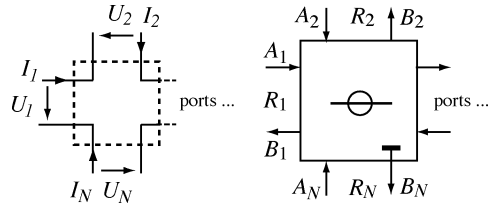

Fig. 4. Series adaptor: (left) connection for K-variables, (right) corresponding WDF symbol for wave variable, including reflection-free port N marked by signal terminal symbol $\top$.

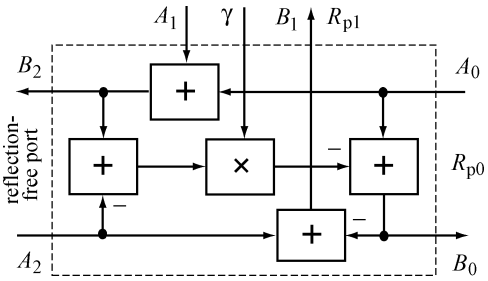

Fig. 5. Three-port series adaptor with a reflection-free port.

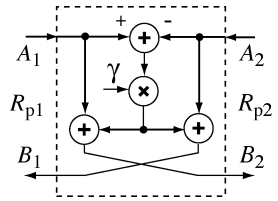

Fig. 6. One-multiplier realization of two-port adaptor.

Fig. 5 shows a computationally efficient realization of a three-port series adaptor.

A useful special case is also the two-port adaptor that can be used to connect two reflection-free ports of different port resistances, shown in Fig. 6, as a one-multiplier realization. It is equivalent to the Kelly–Lochbaum junction, originally proposed for vocal tract modeling in speech synthesis [22]. Here, the scattering coefficient $\gamma = (R_{\text{p2}} - R_{\text{p1}})/(R_{\text{p2}} + R_{\text{p1}})$.

Special multiport adaptors are needed for complex circuit topologies [23], such as the bridge circuit, which are not representable by series and parallel connections.

C. Simple Example of Using Adaptors

A simple example of using adaptors to connect basic WDF elements, applied later in computational efficiency comparison, is depicted in Fig. 7. This resonator circuit is a series connection of an inductor, a capacitor, and a resistor. The WDF circuit is composed as a binary tree where the basic components are at the leaves, and two three-port series adaptors make the port interconnections. The root port on the left of the WDF network is left open, and this reflection-free port can be used for further connections.

D. Basic Two-Port Elements

There are some two-port elements that are important in building WDF models. The *ideal transformer* shown in Fig. 8

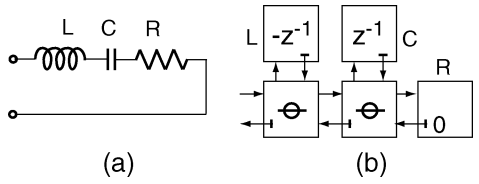

Fig. 7. (a) Series LCR circuit and (b) its WDF realization using three-port series adaptors.

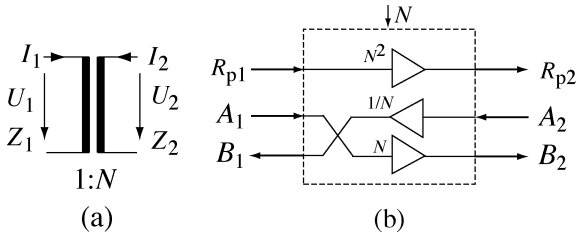

Fig. 8. (a) Ideal transformer and (b) its WDF realization.

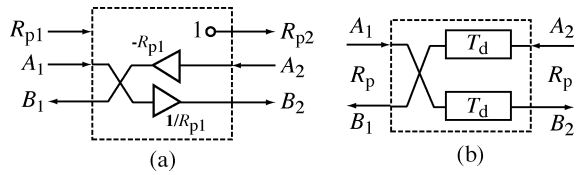

Fig. 9. Two-port WDF elements: (a) dualizer and (b) delay-line.

can be used to change the impedance level of a port to another by "turns ratio" N. It can be realized simply by

$$B_2 = NA_1 \quad \text{and} \quad B_1 = A_2/N \tag{15}$$

$$R_{\mathrm{p}2} = N^2 R_{\mathrm{p}1} \tag{16}$$

so that $Z_2/Z_1 = N^2$.

Another useful port-to-port mapping is by the *gyrator* that maps between capacitive and inductive reactances [10]. Here, we use a specific version of it, the *dualizer*, which transforms an impedance at one port to an admittance at another port or vice versa. The dualizer, depicted in Fig. 9(a), makes the following transform:

$$U_2 = I_1 \quad \text{and} \quad I_2 = -U_1 \tag{17}$$

$$R_{\mathrm{p}2} = 1 \tag{18}$$

so that $Z_2 = 1/Z_1 = Y_1$.

For modeling of signal propagation delays, the original WDF theory contained a unit element [10], in which there are half sample delays to both directions in a bidirectional *delay line*. More generally, we can easily use any computable bidirectional two-port delay line with specified port resistance (wave impedance) as a WDF building element. This includes fractional and variable delays as well [24]. In fact, such delay elements are the basic building blocks of digital waveguides [1]. Fig. 9(b) shows a delay-line two-port element with delay time T_{d} and port resistance R_{p}.

III. Wave-Port Realization of Immittances Given in Various Formats

The basic WDF elements, together with delay lines from the DWG approach, allow for constructing advanced circuit and network structures. On the other hand, it would be convenient to use not only circuits made of the basic WDF elements but also more complex units that simulate given immittances (impedances or admittances) as single consolidated units. An even more important reason to use complex wave-port elements in real-time simulation and sound synthesis is that such consolidated elements are computationally more efficient than circuits built from the basic elements. In this section, we systematically derive a set of such WDF components.

TABLE I
Realization of Basic Parallel and Series Connections of Resistors, Capacitors, and Inductors. Port Resistances R_{p}, Reflectances $H(z)$, and Reflectance Filter Coefficients c and d Are Given. Symbol "$\|$" Means Parallel Connection

Circuit	R_{p}	$H(z)$	c	d
RC ser	$R + R_{\mathrm{C}}$	$z^{-1}\frac{1-c}{1-cz^{-1}}$	R/R_{p}	
RC par	$R \,\|\|\, R_{\mathrm{C}}$	$z^{-1}\frac{1-c}{1+cz^{-1}}$	R_{p}/R	
RL ser	$R + R_{\mathrm{L}}$	$-z^{-1}\frac{1-c}{1+cz^{-1}}$	R/R_{p}	
RL par	$R \,\|\|\, R_{\mathrm{L}}$	$-z^{-1}\frac{1-c}{1-cz^{-1}}$	R_{p}/R	
LC ser	$R_{\mathrm{L}} + R_{\mathrm{C}}$	$z^{-1}\frac{c+z^{-1}}{1+cz^{-1}}$	$\frac{R_{\mathrm{C}}-R_{\mathrm{L}}}{R_{\mathrm{p}}}$	
LC par	$R_{\mathrm{L}} \,\|\|\, R_{\mathrm{C}}$	$-z^{-1}\frac{c+z^{-1}}{1+cz^{-1}}$	$\frac{R_{\mathrm{C}}-R_{\mathrm{L}}}{R_{\mathrm{p}}}$	
LCR ser	$R_{\mathrm{L}} + R_{\mathrm{C}} + R$	$z^{-1}\frac{c+(1-d)z^{-1}}{1+cz^{-1}-dz^{-2}}$	$\frac{R_{\mathrm{C}}-R_{\mathrm{L}}}{R_{\mathrm{p}}}$	$\frac{R}{R_{\mathrm{p}}}$
LCR par	$R_{\mathrm{L}} \,\|\|\, R_{\mathrm{C}} \,\|\|\, R$	$-z^{-1}\frac{c+(1-d)z^{-1}}{1+cz^{-1}-dz^{-2}}$	$\frac{R_{\mathrm{C}}-R_{\mathrm{L}}}{R_{\mathrm{p}}}$	$\frac{R_{\mathrm{p}}}{R}$

A. Series and Parallel Connection of Basic One-Port Elements

Series and parallel connections of resistors, capacitors, and inductors are common cases and, instead of using adaptors like in Fig. 7, we can derive consolidated one-port formulations for them. Port resistance R_{p} and reflectance $H(z)$ for such cases can be derived using (2) and (3). For example, for a series connection of resistance R and inductance L (impedance $Z_{\mathrm{L}}(s) = sL$), we can make the following derivation:

$$Z_{\mathrm{RLser}}(s) = R + sL \tag{19}$$

$$sL = R_{\mathrm{pL}}\frac{1-z^{-1}}{1+z^{-1}} \quad \text{where} \quad R_{\mathrm{pL}} = \frac{2L}{T} \tag{20}$$

$$H_{\mathrm{RLser}}(z) = \frac{R + R_{\mathrm{pL}}(1-z^{-1})/(1+z^{-1}) - R_{\mathrm{p}}}{R + R_{\mathrm{pL}}(1-z^{-1})/(1+z^{-1}) + R_{\mathrm{p}}}. \tag{21}$$

For a reflection-free port

$$R_{\mathrm{p}} = R + R_{\mathrm{pL}} \tag{22}$$

$$H_{\mathrm{RLser}}(z) = \frac{-z^{-1}R_{\mathrm{pL}}/R_{\mathrm{p}}}{1 + (R/R_{\mathrm{p}})z^{-1}} = -z^{-1}\frac{1-c}{1+cz^{-1}} \tag{23}$$

$$c = R/R_{\mathrm{p}}. \tag{24}$$

This means that the reflectance is similar as for the inductor in Fig. 1(d) except that in cascade with $-z^{-1}$ there is a low-pass filter. A similar approach can be applied to other series and parallel connections. Table I lists formulas for the realization of the most common cases.

B. Immittances Given in z-Transform Expressions

In the following, we discuss the means of realizing LTI immittances by FIR and IIR filtering techniques using WDF-com-

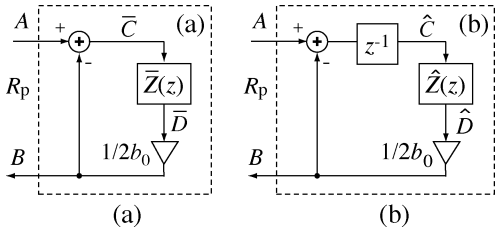

Fig. 10. One-port block made of general impedance according to (25) with subfilter $\bar{Z}(z)$ or $\hat{Z}(z)$.

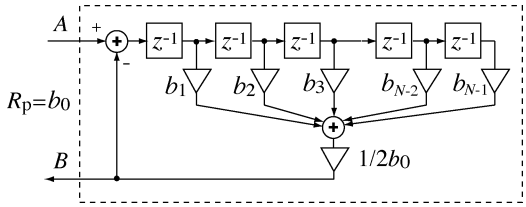

Fig. 11. One-port block with wave port for a given polynomial impedance of (28) to realize the reflectance of (31) and port resistance of (30).

patible wave ports when the immittance is given in a z-transform expression. It is important to remember that immittances given in polynomial or rational z-transform expressions are not filters, although they look like FIR or IIR filters. This is because an impedance is just a constraint between K-variables (e.g., voltage and current), not a causal input–output relationship. It must be converted to a port reflectance to make it a digital filter.

As for the basic WDF elements in Section II, selecting a proper value for port resistance makes the port reflectance free of immediate reflection and thus avoids delay-free loops in WDF networks. If a given impedance $Z(z)$ can be decomposed as

$$Z(z) \Rightarrow b_0 + \bar{Z}(z) = b_0 + z^{-1}\hat{Z}(z) \tag{25}$$

where b_0 is the nondelayed term in expansion $Z(z) = \sum_i b_i z^{-i}$, then, based on (2), the impedance can be realized as a wave port by

$$R_\mathrm{p} = b_0 \tag{26}$$

and

$$H(z) = \frac{\bar{Z}(z)/2b_0}{1+\bar{Z}(z)/2b_0} = \frac{\hat{Z}(z)/2b_0}{1+z^{-1}\hat{Z}(z)/2b_0}z^{-1} \tag{27}$$

as shown in Fig. 10. $Z(z)$ may be specified in various forms, such as a polynomial or rational expression, a parallel or series connection of impedances, or in the form resembling a lattice filter or a frequency-warped [25] filter. In all cases, the filter coefficients or the structures have to be transformed somehow to obtain the modified subfilter $\hat{Z}(z)$ or $\bar{Z}(z)$.

C. Impedance Given in Polynomial Form

Let us first consider the case where an impedance is given as a polynomial form of z-transform expression

$$Z(z) = \frac{U(z)}{I(z)} = \sum_{i=0}^{N-1} b_i z^{-1} \tag{28}$$

where b_i are polynomial coefficients. For compatibility with WDF models, this K-variable expression must be converted to port reflectance $H(z)$ with port resistance R_p by writing

$$H(z) = \frac{Z(z)-R_\mathrm{p}}{Z(z)+R_\mathrm{p}} = \frac{\sum_{i=0}^{N-1} b_i z^{-1} - R_\mathrm{p}}{\sum_{i=0}^{N-1} b_i z^{-1} + R_\mathrm{p}}. \tag{29}$$

We are again interested in realizing the impedance element with a reflection-free port so that it can be used easily in WDF models. It is required that reflection at time index 0 must be zero, which is fulfilled when

$$R_\mathrm{p} = b_0 \tag{30}$$

and

$$H(z) = \frac{\frac{1}{2R_\mathrm{p}}\sum_{i=1}^{N-1} b_i z^{-1}}{1+\frac{1}{2R_\mathrm{p}}\sum_{i=1}^{N-1} b_i z^{-1}}. \tag{31}$$

The reflectance $H(z)$ will therefore be an IIR filter of the same order than the impedance polynomial. Notice also that $b(0)$ must be nonzero to avoid division by zero in (31).

This mapping from $Z(z)$ to $H(z)$ is easy to do, but it would be desirable to use the FIR type expression of $Z(z)$ more directly as a basis for the reflectance as well. The last form of (31) gives a hint about a realization that is close to the FIR filter structure. Fig. 11 shows how the reflectance $H(z)$ can be computed efficiently using the backbone of the regular FIR filter, just slightly modified to make an IIR filter. Only little extra computation is required in comparison to the regular FIR filter form. This formulation results also directly from (27) and Fig. 10(b).

A practical case of finite size polynomial impedance in the acoustical domain is the radiation impedance of a spherical piston in an infinite baffle [26], where a volume velocity impulse results in a finite span force response.

D. Impedance Given in Rational Form

If the impedance $Z(z)$ is given as a rational expression

$$Z(z) = \frac{\sum_{i=0}^{N-1} b_i z^{-i}}{1+\sum_{i=1}^{M-1} a_i z^{-i}} \tag{32}$$

where b_i are numerator and a_i denominator coefficients, the corresponding reflectance $H(z)$ becomes

$$H(z) = \frac{\frac{\sum_{i=0}^{N-1} b_i z^{-i}}{1+\sum_{i=1}^{M-1} a_i z^{-i}} - R_\mathrm{p}}{\frac{\sum_{i=0}^{N-1} b_i z^{-i}}{1+\sum_{i=1}^{M-1} a_i z^{-i}} + R_\mathrm{p}}. \tag{33}$$

A port without delay-free reflection is possible by

$$R_\mathrm{p} = b_0 \tag{34}$$

and

$$H(z) = \frac{\frac{1}{2R_\mathrm{p}}\sum_{i=1}^{N-1} b_i z^{-i} - \frac{1}{2}\sum_{i=1}^{M-1} a_i z^{-i}}{1+\frac{1}{2R_\mathrm{p}}\sum_{i=1}^{N-1} b_i z^{-i} + \frac{1}{2}\sum_{i=1}^{M-1} a_i z^{-i}}. \tag{35}$$

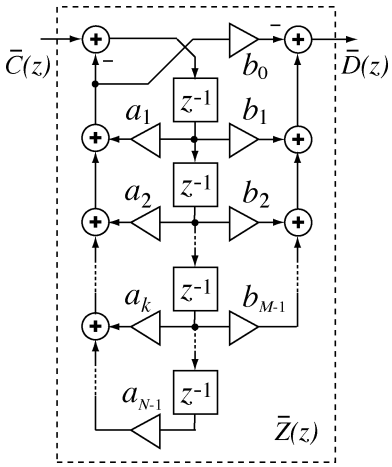

Fig. 12. Subfilter $\bar{Z}(z)$ according to (25) and Fig. 10(a) to realize a wave port for impedance $Z(z)$ as specified by a rational expression in (32).

When the coefficients in (35) are processed, a regular IIR filter (without a b_0-term) is obtained for the reflectance as

$$H(z) = \frac{\sum_{i=1}^{N-1} b'_i z^{-i}}{1 + \sum_{i=1}^{N-1} a'_i z^{-i}} \tag{36}$$

$$b'_i = (b_i - a_i b_0)/2b_0 \tag{37}$$

$$a'_i = (b_i + a_i b_0)/2b_0. \tag{38}$$

It would be useful to formulate the reflectance so that it is based on the original coefficients of impedance specification without need of modifications, like it was done for the polynomial impedance. This is possible by using the rule of (25)

$$\bar{Z}(z) = \frac{\sum_{i=0}^{N-1} b_i z^{-i}}{1 + \sum_{i=1}^{M-1} a_i z^{-i}} - b_0 \tag{39}$$

$$= \frac{\sum_{i=1}^{N-1} (b_i - a_i b_0) z^{-i}}{1 + \sum_{i=1}^{M-1} a_i z^{-i}}. \tag{40}$$

Applying this to Fig. 10 with minor rearrangements results in the realization of the subfilter $\bar{Z}(z)$ as shown in Fig. 12.

E. Second-Order Sections

An important special case of rational discrete-time forms is the second-order section, in which case impedance is given as

$$Z(z) = \frac{b_0 + b_1 z^{-1} + b_2 z^{-2}}{1 + a_1 z^{-1} + a_2 z^{-2}}. \tag{41}$$

According to (36), the reflectance becomes

$$H(z) = \frac{b'_1 z^{-1} + b'_2 z^{-2}}{1 + a'_1 z^{-1} + a'_2 z^{-2}} \tag{42}$$

where mapped coefficients b'_i and a'_i are according to (37) and (38) for $i = 1$ and 2.

The original rational coefficients can be kept by applying the principle of (25)–(27) and Fig. 10 so that the subfilter $\bar{Z}(z)$ becomes

$$\bar{Z}(z) = \frac{(b_1 - a_1 b_0) z^{-1} + (b_2 - a_2 b_0) z^{-2}}{1 + a_1 z^{-1} + a_2 z^{-2}}. \tag{43}$$

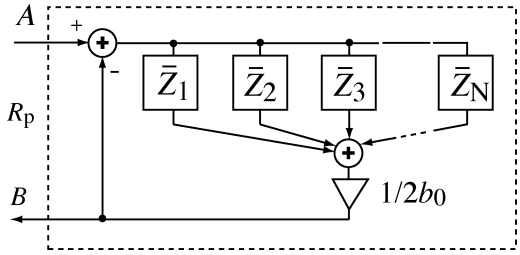

Fig. 13. One-port block with wave port for impedance given as a combination of subfilters $\bar{Z}_k(z)$ for series connection of impedances.

It can be realized by using a second-order version of subfilter shown in Fig. 12.

F. Impedance Given in Series Form

High-order filters are often realized as series or parallel connections of second-order sections, which is numerically more robust than using corresponding high-order direct form filters. The same holds for the computation of impedances as well. A series connection of second-order impedance terms is specified as

$$Z_{\text{ser}}(z) = \sum_{k=0}^{N-1} Z_k(z) = \sum_{k=0}^{N-1} \frac{b_{0,k} + b_{1,k} z^{-1} + b_{2,k} z^{-2}}{1 + a_{1,k} z^{-1} + a_{2,k} z^{-2}}. \tag{44}$$

Notice that a series connection of impedances is realized by a form that looks like a parallel connection of filters. Form (44) can be mapped to reflectance in various ways following the rules applied above, but here we are interested particularly in a formulation where the sections can be realized separately and where the original coefficients can be used without transformations. It is now obvious that delay-free loops can be avoided when

$$R_{\text{p}} = \sum_{k=0}^{N-1} b_{0,k}. \tag{45}$$

By inserting $b_0 = R_{\text{p}}$ from (45) and (44) into (25), we can notice that $\bar{Z}(z)$ will be the sum of second-order subfilters $\bar{Z}_k(z)$ specified by (43) and a second-order version of Fig. 12, resulting in the realization of Fig. 13.

G. Impedance Given in Parallel Form

Parallel connection of impedances turns out to be inconvenient for finding a solution similar to the serial connection because the parallel connection formula

$$Z_{\text{par}}(z) = \frac{1}{\sum_{k=0}^{N-1} 1/Z_k(z)} = \frac{1}{\sum_{k=0}^{N-1} Y_k(z)} \tag{46}$$

is difficult to work out to a consolidated wave port having the original parameter coefficients. Parallel connection of admittances is, however, a dual structure to impedances in series, so the denominator of (46) is easy to realize as the sum of admittances $Y_k(z)$, which are reciprocals of the impedances $Z_k(z)$. The consolidated admittance can finally be converted to corresponding impedance by using the dualizer of (17) and Fig. 9(a), which requires only two extra multiplications for LTI models

with constant port resistances. This case shows how it is convenient to operate with the concept of duality between variables, element types, and series versus parallel structures.

H. Impedance Given in State-Space Form

Petrausch and Rabenstein [19] have studied the K-to-W conversion for making WDF-compatible wave ports using the state-space formalism. It is obvious that the conditions of making reflection-free wave ports are conceptually the same as in this paper, since they must be based on the mapping in (2), and therefore the two approaches must lead to functionally equivalent results. However, no analysis of computational optimization and implementation efficiency is presented in [19].

I. Modal Decomposition of Admittances

As an example of practical modeling of a driving-point admittance in the mechanical domain, modal decomposition of a given admittance as a wave port is discussed briefly. A classical formulation of mechanical admittance (also called mobility) [27], when using the Laplace transform variable s instead of $j\omega$, is

$$Y(s) = \sum_k \frac{s}{m_k\,(s^2 + s\omega_k/Q_k + \omega_k^2)} \tag{47}$$

where k is the mode index, m_k is the mode-related effective mass, ω_k is the angular frequency of the mode, and Q_k its Q-value. Equation (3) can be used to map the admittance to the z-domain so that

$$Y(z) = \sum_k \frac{b'_{0,k}(1 - z^{-2})}{1 + a'_{1,k}z^{-1} + a'_{2,k}z^{-2}} \tag{48}$$

$$b'_{0,k} = \frac{2/m_k T}{\omega_k^2 + 2\omega_k/Q_k T + 4/T^2} \tag{49}$$

$$a'_{1,k} = -\frac{8/T^2}{\omega_k^2 + 2\omega_k/Q_k T + 4/T^2} \tag{50}$$

$$a'_{2,k} = \frac{4/T^2 - 2\omega_k/Q_k T}{\omega_k^2 + 2\omega_k/Q_k T + 4/T^2}. \tag{51}$$

This mapping brings along the frequency warping of (4). This undesirable feature can be counteracted by frequency prewarping applied to ω_k in the analog domain using (4) before mapping to the discrete-time domain. Another possibility is to use oversampling so that warping in the baseband remains below an acceptable limit.

As can be concluded from (48)–(51) and the need to compensate for frequency warping, the computation of filter reflectance coefficients from physical parameters becomes complicated particularly for real-time updating. The impulse invariant mapping [20] is another alternative, where the warping can be avoided, but it brings the problem of additional losses (limited Q-values) when the modal resonance is at high frequencies, and the parameter mapping needed is still quite complex. These facts make the impulse invariant mapping useless in high-Q applications.

Instead of bilinear and impulse invariant mapping, a useful approximation for high-Q modal resonances in (47), found semi-experimentally to combine features from the two methods, is

$$b'_{0,k} = (1 - r_k)Y_{k,\mathrm{res}} \tag{52}$$

$$a'_{1,k} = -2r_k \cos(\Omega_k) \tag{53}$$

$$a'_{2,k} = r_k^2 \tag{54}$$

$$r_k = 1 - \Omega_k/(2Q_k) \tag{55}$$

$$\Omega_k = 2\pi f_k/f_\mathrm{s} \tag{56}$$

where f_s is the sample rate and control parameters are f_k for the modal resonance frequency, Q_k for the Q-value of the resonance, and $Y_{k,\mathrm{res}} = Q_k/(m_k\omega_k)$ for the modal admittance at the resonance frequency according to (47). For $Q > 10$, this approximates the resonance peak frequency and response decay rate with accuracy of 0.1% and peak magnitude of admittance with accuracy of 0.5 dB within 20–15 000 Hz for the sample rate of 44 100 Hz.

Admittance $Y(z)$ is often obtained directly in the z-domain based on parametric matching to measurement data, for example to the form of (48). The series connection technique of Section III-F can be used for realization of the consolidated admittance and a dualizer to map it to an impedance port.

TABLE II
COMPUTATIONAL EFFICIENCY COMPARISON OF REGULAR AND CONSOLIDATED WDF STRUCTURE USING (A) MULTIPLICATION AND ADDITION OPERATIONS, (B) MULTIPLY-ACCUMULATE OPERATIONS, AND (C) C PROGRAM EFFICIENCY (1 MILLION STEPS)

Realization	mul + add	MAC	CPU time
Standard WDF	2 + 8 = 10	10	0.035 s
Consolidated	4 + 3 = 7	4	0.0185 s

IV. IMPLEMENTATION ISSUES

In this section, we present a straightforward analysis of computational efficiency of the proposed consolidated wave-port filter structures against the realization using basic WDF building blocks. Comments on the algorithmic accuracy and robustness of various formulations are also given based on programming experiences.

A. Computational Efficiency Analysis

The efficiency of the proposed approach is analyzed here using some concrete examples. Because the detailed efficiency of each algorithm depends on the instruction architecture of the processor used, the comparison is first based on the number of basic operations, particularly of additions (or subtractions) and multiplications, or multiplication-accumulation (MAC) operations. Another comparison is done based on C program testing. The model parameters are assumed to have constant values so that they do not need updating.

1) LCR Circuit Performance: The first case is a series LCR circuit as presented in Fig. 7 as a standard WDF network (L + C + R + 2 adaptors as shown in Fig. 5) and for the consolidated one-port element [second-order filter of (42)]. By counting the basic operations, we get the comparison of Table II.

The difference is not big when using separate additions and multiplications, but with MAC instructions, the consolidated model needs only 40% of the standard WDF instructions. In

both cases, the overhead due to memory references is not taken into account.

Table II compares also the execution times evaluated on a 1.67-GHz PowerPC processor when both cases have been programmed in the C language and compiled using the gcc compiler [28]. In this case, the consolidated realization needs about 53% of the CPU time compared to the standard WDF model. The execution times are for 1 million repetitions of the code, loop overhead not included.

2) Parallel Modal Waveport: From the comparisons above, it can be estimated that approximately the same performance ratios are valid also for the modal decomposition structures of Section III-I, because they are made of second-order sections connected in parallel.

3) Polynomial and Rational Impedance Performance: The polynomial impedance realization in Fig. 11 can be easily seen to be roughly twice as fast to compute as the general IIR form of (31) that is not utilizing the structural redundancy, as it is found between an FIR and an IIR filter of the same order in general. For the case of rational impedance formulation, this advantage is not gained because the order of filter is preserved. The advantage of using the original filter coefficients is retained, however; see Fig. 12.

B. Accuracy and Robustness

The key concept of this paper is the tradeoff between robustness of basic WDFs and efficiency of the consolidated components. Wave digital filters composed of the basic elements through adaptor interconnections are known for their excellent numerical robustness [10]–[14], which is common to many W-modeling methods in general. Consolidation of the model structures improves computational efficiency, but the price paid is that numerical robustness generally decreases. Notice that for infinite numerical precision, consolidated components based on mapping (3) would in LTI cases behave equivalently to the classical WDFs, and therefore passivity and stability conditions are the same.

The question arises of how to state the stability conditions for the consolidated components. For example, the polynomial immittance formulation in III-C deviates conceptually from the classical thinking, where passivity is guaranteed by the property of immittances being positive-real [29], which in case of basic WDF elements can be met easily. For consolidated components the positive-realness can be checked out numerically, in most cases not being a serious problem in practice. It is also a fact that in many models with inherently high losses (low Q-value), stability is easily achieved. Furthermore, other mappings from the Laplace domain than the bilinear one may be found useful or even better in some cases.

The rules to evaluate the numerical accuracy of filters in consolidated components follow the general rules for different digital filter topologies. For example, a second-order section of filter in (32) is critical in floating-point computation only when the Q-value of a resonance becomes extremely high. With double-float precision on a PowerPC processor, second-order sections were tested to remain robust beyond $Q > 100\,000$ and for single-float precision up to about $Q \sim 20\,000$ for the entire audio range (20–20 000 Hz) with sample rate of 44 100 Hz.

On the other hand, consolidation of many high-Q resonances using the rational impedance realization of Fig. 12 becomes easily impossible with any practical numerical precision. A good compromise between efficiency and robustness is achieved by the series impedance structure of III-F.

C. Implementation in Modeling Software

There exist only few generic software tools for true physical modeling with two-way interaction between components. Binary connection tree (BCT) [30] is an example of a WDF modeling tool. We have been developing a software platform called BlockCompiler [31], [32] that is a hybrid modeling environment supporting WDFs, DWGs, and other paradigms, including also DSP modeling with one-directional interaction between signal terminals. BlockCompiler is basically a code generator that produces C language code from models (patches) built from blocks and compiles the code into efficient executables for real-time simulation. The principles and cases discussed in this paper have been implemented and tested in BlockCompiler.

V. Modeling Example

As an example case, we develop a "semiphysical" model of a bell for sound synthesis. It is based on earlier work presented in [33], using recorded data from a real bell.[2] This application case is somewhat trivial because it can be easily simulated as well by straightforward DSP filtering for modal resonances, but it was found a good example to demonstrate an efficient realization of a numerically demanding high-Q model without problems in accuracy and stability.

Bells are physical objects that, as 3-D structures, have an inharmonic spectrum of partials, some of them made approximately harmonic by proper design [34]. Each partial may actually consist of two or more eigenmodes that are typically slightly off-tuned in frequency due to some asymmetry, which creates beating (warble) in the temporal envelope.

In a full physical model, a bell should be represented as a spatially distributed system, excited by hammering at some position, and sound radiating from all of its surfaces. For real-time sound synthesis, the bell model needs to be simplified, yet retaining the most important physical and perceptual features. In our case, we reduce the model into a single wave port, where the hammer excitation as well as sound radiation take place. This makes it possible to use for example a nonlinear hammer model, although such analysis remains outside the scope of the paper.

The bell recording was analyzed by the FZ-ARMA method proposed in [35], a technique for high-resolution analysis to get accurate estimates of parameters for high-Q modes even when they are very near or overlapping in frequency. The method was applied directly to the recorded bell sound. Table III shows the modal data obtained up to 10 kHz, so that each partial was assumed to consist of two eigenmodes. As can be noticed, very high Q-values (up to about 10 000) of modal resonances are found.

A synthesis model was constructed from the modal data using the modal synthesis method of (52)–(56) with good results. The wave port was realized simply as a series connection, according to Fig. 13, of second-order admittance sections using the subfilter structure in Fig. 12. The port admittance (mobility) was

[2]A bell from the Belfort bell recordings provided by M. Leman.

TABLE III
MODAL DATA FOR THE BELL OF THE CASE STUDY INCLUDING TWO MODES PER PARTIAL: MODE FREQUENCIES (f_1 AND f_2), Q-VALUES (Q_1 AND Q_2), AND MODE ADMITTANCES ($Y_{\mathrm{res},1}$ AND $Y_{\mathrm{res},2}$) ARE GIVEN

k	f_1/Hz	Q_1	$Y_{\mathrm{res},1}$	f_2/Hz	Q_2	$Y_{\mathrm{res},2}$
1	850.8	880	0.0723	851.3	4007	0.0965
2	1702.3	4968	0.1497	1703.1	4507	0.0514
3	2026.7	4521	0.1258	2032.8	612	0.0734
4	2787.2	2294	0.0763	2792.5	1387	0.0364
5	3404.7	5375	0.0610	3407.0	2107	0.0716
6	4552.1	793	0.0290	4559.6	3163	0.0278
7	4889.6	4565	0.0554	5050.5	8205	0.0511
8	6881.5	6421	0.1261	6889.2	2184	0.0088
9	8549.8	8232	0.0029	8631.9	1257	0.0047
10	8695.0	5939	0.0313	8842.0	8509	0.0191

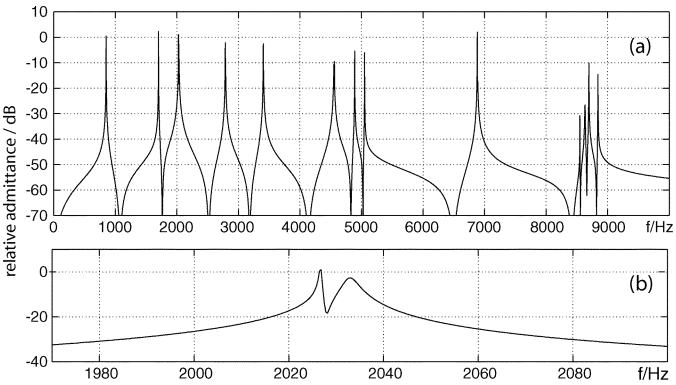

Fig. 14. (a) Synthesized bell port admittance (dB-scaled) as a function of frequency and (b) zooming to the details of the third partial.

"measured" by connecting the port to an impulse force source and observing the port velocity. Fig. 14(a) plots the magnitude of admittance as a function of frequency. Zooming to the third partial is shown in Fig. 14(b), indicating the need of high spectral resolution to produce the beating effect due to nearby modes.

The bell model synthesized by the modal decomposition sounds very realistic when compared to the original recording, only recording noise and acoustic environment reverberation are reduced. An interesting observation found is that a single prototype bell can be used to obtain high-quality bell sounds within plus or minus one octave of frequency scaling, applied linearly to all modal frequencies.

Based on the performance analysis in Section IV-A1, up to about 40 such bell model ports, each with 12 partials (24 modes, in average per model), can be computed concurrently in real time at the sample rate of 44 100 Hz on a PowerPC 1.67-GHz processor.

VI. DISCUSSION AND CONCLUSION

This paper has shown how to consolidate WDF structures made of basic wave digital filter elements into computationally more efficient wave port components. By proper filter topologies, the original coefficients can often be used as such without need to transform them. The rules for making such consolidated wave ports cover immittances given by polynomial or rational z-transform formulations as well as series and parallel connections of arbitrary immittances. Furthermore, modal decomposition of driving-point immittances has been discussed briefly. Immittances given in analog (continuous-time) specification can be mapped to a z-transform formulation using the bilinear transform.

Together, these techniques enable efficient physics-based modeling of a wide variety of LTI systems, for example in the electrical, mechanical, and the acoustical domains. A rule of thumb for efficiency improvement using consolidated components instead of classical WDF elements is about 50% savings in CPU time on general-purpose processors. Computation speed is often of main importance in sound synthesis, as far as numerical robustness is fulfilled. A case study of bell modeling has been presented to demonstrate efficient real-time sound synthesis without sacrificing robustness.

Consolidated wave port components are particularly useful in modeling when an analog immittance prototype is not available at all. Examples thereof are cases where a z-transform expression is the starting point, such as when it is derived from measurements and parametric fitting of a polynomial or rational form to the data. This is a common case for example in modeling complex subsystems of musical instruments.

Consolidated components are found useful also for complex circuit topologies that cannot be decomposed by using series and parallel adaptors. One such problem is found in "virtual analog" modeling of classical guitar amplifier circuits: the tone stacks (tone controls), which contain bridge circuits [23]. Direct WDF modeling leads to complex multiport adaptors and even more complex parameter updating [36]. The Delta-to-Wye and Wye-to-Delta circuit transforms [37] result in components that can be realized in consolidated form, which simplifies the solution of the problem. Further discussion of such techniques is out of the scope of this paper.

The cost often paid for increased efficiency is the reduction of numerical robustness. WDFs made of basic elements and adaptors are known for their excellent numerical properties, which can easily be lost by excessive consolidation of the structures. However, by keeping the complexity of wave port components to second-order structures and their combinations, not much is sacrificed so that particularly with double precision floating-point computation, the numerical accuracy requirements are easily fulfilled. On the other hand, if only short word-length integer arithmetic is available, the requirements on numerical robustness may in most cases make consolidation useless.

Another limitation introduced by consolidation is that there is no direct access to the K- or W-variables of the constituent elements; only the consolidated port can be observed directly. A further question with consolidation is possible problems in time-varying and nonlinear modeling. If the rate of change of filter parameters is slow enough, for example below the audible frequency range for audio applications, this may not be a problem. For rapidly changing parameters or strong nonlinearities, such consolidation may not work, leading to violation of energy preservation rules and stability of models. In such cases, careful physical modeling using the basic WDF elements is needed with the price paid for increased computational load.

Among topics for future research are for example more detailed formulation of specific cases and generalization of the principles to consolidated two-port and multiport elements. As an example, the guitar bridge is in fact a multiport, where not only driving-point admittances but also transfer admittances between different strings and polarizations of a single string need

to be explicated in detailed modeling. This brings some new realization questions although the main principles remain much the same.

ACKNOWLEDGMENT

The author would like to thank B. Bank, D. Yeh, J. Pakarinen, and C. Erkut for valuable comments on the manuscript.

REFERENCES

[1] J. O. Smith, *Physical Audio Signal Processing: Digital Waveguide Modeling of Musical Instruments and Audio Effects,* 2004. [Online]. Available: http://ccrma.stanford.edu/~jos/pasp/, Aug. 2006 Edition

[2] V. Välimäki, J. Pakarinen, C. Erkut, and M. Karjalainen, "Discrete-time modelling of musical instruments," *Rep. Progress in Phys.*, vol. 69, pp. 1–78, Jan. 2006.

[3] S. Bilbao, *Wave and Scattering Methods for Numerical Simulation*. New York: Wiley, 2004.

[4] S. A. Van Duyne, J. R. Pierce, and J. O. Smith, "Traveling-wave implementation of a lossless mode-coupling filter and the wave digital hammer," in *Proc. Int. Comput. Music Conf.*, Aarhus, Denmark, 1994, pp. 411–418.

[5] F. Pedersini, A. Sarti, and S. Tubaro, "Block-wise physical model synthesis for musical acoustics," *Electron. Lett.*, vol. 35, pp. 1418–1419, Aug. 1999.

[6] J. Bensa, S. Bilbao, R. Kronland-Martinet, and J. O. Smith, "A power normalized non-linear lossy piano hammer," in *Proc. Stockholm Music Acoust. Conf.*, Stockholm, Sweden, Aug. 6–9, 2003, vol. I, pp. 365–368.

[7] M. van Walstijn and G. P. Scavone, "The wave digital tonehole model," in *Proc. Int. Comput. Music Conf.*, Berlin, Germany, 2000, pp. 465–468.

[8] D. Fränken, K. Meerkötter, and J. Waßmuth, "Passive parametric modeling of dynamic loudspeakers," *IEEE Trans. Speech Audio Process.*, vol. 8, no. 8, pp. 885–891, Nov. 2001.

[9] M. Karjalainen and J. Pakarinen, "Wave digital simulation of a vacuum-tube amplifier," in *Proc. IEEE ICASSP'06*, Toulouse, France, May 15–19, 2006, pp. V-153–V-156.

[10] A. Fettweis, "Wave digital filters: Theory and practice," *Proc. IEEE*, vol. 74, no. 2, pp. 270–327, Feb. 1986.

[11] A. Fettweis, "Pseudopassivity, sensitivity, and stability of wave digital filters," *IEEE Trans. Circuit Theory*, vol. CT-19, no. 6, pp. 668–673, Nov. 1972.

[12] A. Fettweis, "On sensitivity and roundoff noise in wave digital filters," *IEEE Trans. Acoust., Speech, Signal Process.*, vol. 22, no. 5, pp. 383–384, Oct. 1974.

[13] K. Ochs, "Passive integration methods: Fundamental theory," *Int. J. Electron. Commun. (AEÜ)*, vol. 55, pp. 153–163, May 2001.

[14] D. Fränken and K. Ochs, "Numerical stability properties of passive Runge–Kutta methods," in *Proc. IEEE Int. Symp. Circuits, Syst. (ISCAS)*, Sidney, Australia, May 2001, pp. 473–476.

[15] K. Meerkötter and R. Scholz, "Digital simulation of nonlinear circuits by wave digital filters," in *Proc. IEEE Int. Symp. Circuits Syst. (ISCAS)*, 1989, pp. 720–723.

[16] A. Sarti and G. De Poli, "Toward nonlinear wave digital filters," *IEEE Trans. Signal Process.*, vol. 47, no. 6, pp. 1654–1668, Jun. 1999.

[17] K. Manivannan, C. Eswaran, and A. Antoniou, "Design of low-sensitivity universal wave digital biquads," *IEEE Trans. Circuits Syst.*, vol. 36, no. 1, pp. 108–113, Jan. 1989.

[18] D. Rocchesso and J. O. Smith, "Generalized digital waveguide networks," *IEEE Trans. Speech Audio Process.*, vol. 11, no. 3, pp. 242–254, May 2003.

[19] S. Petrausch and R. Rabenstein, "Interconnection of state space structures and wave digital filters," *IEEE Trans. Circuits Syst., Part II (Express Briefs)*, vol. 52, no. 2, pp. 90–93, Feb. 2005.

[20] J. G. Proakis and D. G. Manolakis, *Digital Signal Processing—Principles, Algorithms, and Applications*, 4th ed. Upper Saddle River, NJ: Pearson Prentice-Hall, 2007.

[21] A. G. Constantinides, "Spectral transformations for digital filters," *Proc. Inst. Elect. Eng.*, vol. 117, no. 8, 1970.

[22] J. L. Kelly and C. C. Lochbaum, "Speech synthesis," in *Proc. 4th Int. Congr. Acoust.*, Copenhagen, Denmark, Sep. 1962, pp. 1–4.

[23] D. Fränken, J. Ochs, and K. Ochs, "Generation of wave digital structures for networks containing multiport elements," *IEEE Trans. Circuits Syst.*, vol. 52, pp. 586–596, Mar. 2005.

[24] T. I. Laakso, V. Välimäki, M. Karjalainen, and U. K. Laine, "Splitting the unit delay—Tools for fractional delay filter design," *IEEE Signal Process. Mag.*, vol. 13, pp. 30–60, Jan. 1996.

[25] M. Karjalainen, A. Härmä, and U. K. Laine, "Relizable warped iir filters and their properties," in *Proc. IEEE ICASSP'97*, Munich, Germany, Apr. 21–24, 1997, vol. 3, pp. 2205–2208.

[26] L. L. Beranek, *Acoustics*. Melville, NY: American Inst. of Phys., 1988, 3rd printing.

[27] T. J. W. Hill, B. E. Richardson, and S. J. Richardson, "Acoustical parameters for the characterisation of the classical guitar," *Acta Acustica United With Acustica*, vol. 90, no. 2, pp. 335–348, 2004.

[28] "GCC, the GNU compiler collection," [Online]. Available: http://gcc.gnu.org/

[29] M. E. V. Valkenburg, *Introduction to Modern Network Synthesis*. New York: Wiley, 1960.

[30] G. De Sanctis, A. Sarti, and S. Tubaro, "Automatic synthesis strategies for object-based dynamical physical models in musical acoustics," in *Digital Audio Effects (DAFx'03)*, London, U.K., Sep. 8–11, 2003, pp. 219–224.

[31] M. Karjalainen, "BlockCompiler: Efficient simulation of acoustic and audio systems," in *Proc. 114th AES Conv.*, Amsterdam, The Netherlands, Mar. 22–25, 2003.

[32] "BlockCompiler Web Page." [Online]. Available: http://www.acoustics.hut.fi/software/BlockCompiler/

[33] M. Karjalainen, J. Pakarinen, C. Erkut, P. A. A. Esquef, and V. Välimäki, "Recent advances in physical modeling with K- and W-techniques," in *Proc. Digital Audio Effects (DAFX'04)*, Naples, Italy, Oct. 5–8, 2004, pp. 107–112.

[34] N. H. Fletcher and T. D. Rossing, *The Physics of Musical Instruments*. New York: Springer-Verlag, 1991.

[35] M. Karjalainen, P. A. A. Esquef, P. Antsalo, A. Mäkivirta, and V. Välimäki, "Frequency-zooming ARMA modeling of resonant and reverberant systems," *J. Audio Eng. Soc.*, vol. 50, no. 12, pp. 953–967, 2002.

[36] D. Yeh and J. O. Smith, "Discretization of the '59 Fender Bassman tone stack," in *Proc. DAFx-06*, Montreal, QC, Canada, Sep. 18–20, 2006, pp. 1–5.

[37] J. W. Nilsson and S. A. Riedel, *Electric Circuits*, 6th ed. Upper Saddle River, NJ: Prentice-Hall, 1999.

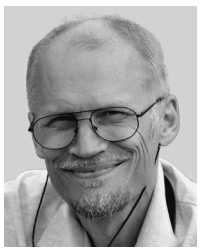

Matti Karjalainen (M'84–SM'01) was born in Hankasalmi, Finland, in 1946. He received the M.Sc. and Dr.Sc. (Tech.) degrees in electrical engineering from the Tampere University of Technology, Tampere, Finland, in 1970 and 1978, respectively.

Since 1980, he has been a Professor in acoustics and audio signal processing at the Helsinki University of Technology, Espoo, Finland, in the Department of Electrical and Communications Engineering. In audio technology, his main interest is in audio signal processing, such as DSP for sound reproduction and auralization, music DSP and sound synthesis, as well as perceptually based signal processing. In addition to audio DSP, his research activities cover speech processing, perceptual auditory modeling and spatial hearing, DSP hardware, software, and programming environments, as well as various branches of acoustics, including musical acoustics and modeling of musical instruments.

Prof. Karjalainen is an Audio Engineering Society Fellow and silver medalist and member of the Acoustical Society of America, European Acoustics Association, International Speech Communication Association, and several Finnish scientific and engineering societies.